Clin Neuroradiol (2019) 29:383–389
https://doi.org/10.1007/s00062-019-00791-3

CLINICAL CASE

Freiburg Neuropathology Case Conference: a Hemorrhagic Intraspinal Tumor Extending from L3 to S1

C. A. Taschner[1] · M. Schwabenland[2] · U. Hubbe[3] · H. Urbach[1] · A. Stadler[1] · M. Prinz[2,4,5]

Published online: 22 May 2019

Keywords Spinal metastasis · Spinal meningioma · Myxopapillary ependymoma · Spinal paraganglioma · Schwannoma

Case Report

A 58-year-old male presented to the emergency department with severe back pain. He had fallen on his hip the same day. He immediately experienced severe back pain which was not apparent before. He reported a history of impaired bladder control and fecal incontinence for more than 1 year. Due to pre-existing mental retardation the patient could not give reliable information concerning esthesia but seemed to feel pain proximal to his knees but not his feet. He suffered severe paresis of the psoas muscles and the quadriceps muscles (grade 2/5 both sides) and a complete paralysis of the distal leg muscles. Computed tomography (CT) and magnetic resonance imaging (MRI) were done the same day and revealed an intraspinal mass extending from L3 to S1. Due to the high-grade neurological deficits an emergency open biopsy was performed. After a medial skin incision, a right-sided interlaminar fenestration was performed including a resection of the L2/3 facet joint. After removal of the ligamentum flavum the dura was found to be under pressure from livid material compatible with a hematoma. There was no epidural hematoma. After longitudinal incision of the dura reddish tumor material with high bleeding tendency was found and removed for histopathological examination. It was not possible to delimit the fascicles of the cauda equina within the mass lesion. Preliminary histopathological examination only revealed signs of hematoma within the specimens that had been sent to pathology. Therefore, further epidural preparation to the anterior spinal canal was performed, where more tumor material with epidural compression of the dura was found. Here the preliminary histopathological examination revealed a metastasis or a plasmacytoma as most likely diagnoses. Therefore, no further resection was performed and closure of the approach was performed in layers. Postoperatively the patient showed gradual worsening of the paresis with nearly complete paralysis now also of the quadriceps and the psoas bilaterally (grade 1/5). Postoperative MRI showed signs of a circumscribed decompression at the L2/3 level on the right side and no signs of a new intraspinal bleeding. With respect to the tumor, no possibilities could be seen for further decompression or resection due to the massive hemorrhage and the high vascularization of the tumor tissue. Concerning the instability of the lower lumbar spine and the lumbosacral junction including S1, however, a stabilization was indicated and performed 3 days after the biopsy. Postoperatively the patient showed no additional deficits and during the following days no wound healing problems occurred and he reported an improvement of the sensitivity while the paresis remained stable.

Imaging

Sagittal T2-weighted images (Fig. 1a) showed a huge intraspinal and intradural mass lesion extending from L3 through to S1 (arrow). The vertebrae at the corresponding levels were destroyed. The signal intensity of the tumor mass was homogeneously isointense. Mind the fluid-fluid level depicted (arrowhead) corresponding to an intraspinal haemorrhage. On T1 weighted images the tumor

✉ C. A. Taschner
christian.taschner@uniklinik-freiburg.de

1 Department of Neuroradiology, Medical Center, Faculty of Medicine, University of Freiburg, Breisacherstraße 64, 79106 Freiburg, Germany

2 Institute of Neuropathology, Faculty of Medicine, University of Freiburg, Freiburg, Germany

3 Department of Neurosurgery, Medical Center, Faculty of Medicine, University of Freiburg, Freiburg, Germany

4 Centers for Biological Signalling Studies BIOSS and CIBSS, University of Freiburg, Freiburg, Germany

5 Center for NeuroModulation, Faculty of Medicine, University of Freiburg, Freiburg, Germany

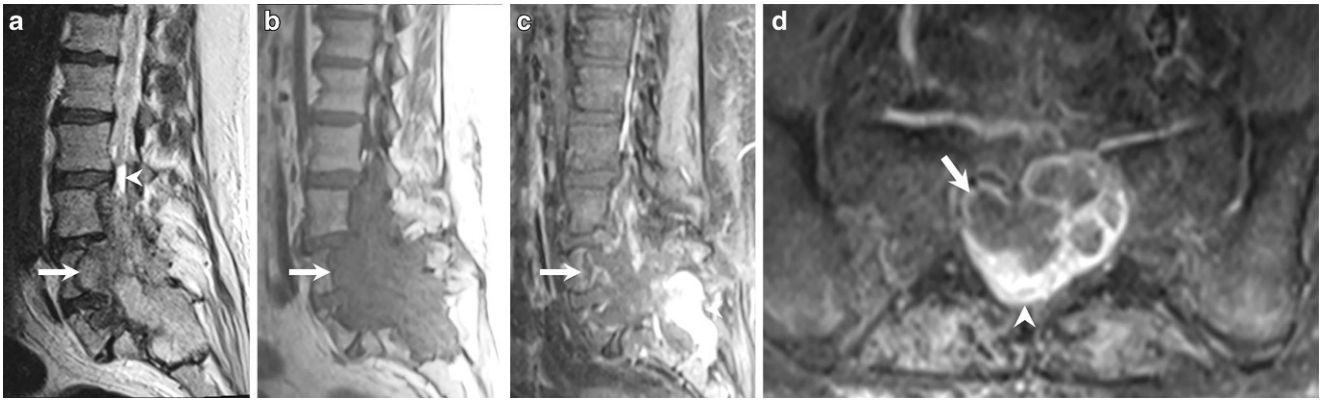

Fig. 1 Sagittal T2-weighted image (**a**) showing a huge intraspinal and intradural mass lesion extending from L3 through to S1 (*arrow*). The vertebrae at the corresponding levels are destroyed. The signal intensity of the tumor mass is homogeneously isointense. Fluid-fluid level depicted (*arrowhead*) were interpreted as intraspinal hemorrhage. On sagittal T1-weighted images (**b**) the tumor appears homogeneously hypointense. On sagittal (**c**) and coronal (**d**) T1-weighted images after i.v. administration of gadolinium the lesion (arrow) reveals an inhomogeneous pattern of enhancement. At the levels L3–4 the lesion shows a capsular type of enhancement with apparent regressive changes in the center. At the level L5-S1 the lesion reveals compact tumor matrix with marked and homogeneous contrast enhancement (**c** + **d**, *arrowhead*)

Fig. 2 On CT scan in bone window settings, the tumor shows massive destruction of the vertebrae L3 through to S1 (*arrow*). The tumor seems to have a slowly progressing growth pattern, since a sclerotic rim is present (*arrowhead*)

appeared homogeneously hypointense (Fig. 1b, arrow). On T1-weighted images after i.v. administration of gadolinium, the lesion (Fig. 1c, arrow) revealed an inhomogeneous pattern of enhancement. At the levels L3–4 the lesion showed a capsular type of enhancement with apparent regressive changes in the center. At the level L5-S1 the lesion revealed a compact tumor matrix with marked and relatively homogeneous contrast enhancement (Fig. 1c and d, arrowhead). On CT scan in bone window settings, the tumor showed massive destruction of the vertebrae L3 through to S1 (Fig. 2, arrow). The tumor seemed to have a slowly progressing growth pattern, since a sclerotic rim was present (Fig. 2 arrowhead).

Differential Diagnosis

Metastases

Metastases, either lytic or sclerotic, are the most frequent bone malignancies and up to 80% are due to breast, prostate, thyroid, lung and kidney carcinomas. Predilection sites for osseous metastases are all segments of the spine, skull and ribs. Bone marrow is invaded early, while cortical destruction with fractures and/or intraspinally and extraspinally growing mass leading to compression of the spinal cord and extravertebral structures occurs later. The CT findings of an osteolytic lesion are replacement of normal osseous trabeculae, cortical destruction and possibly pedicular destruction and a paravertebral mass with contrast enhancement [1–3]. The MRI findings are typically T1-weighted hypointensity because of replacement of the usual hyperintense adult bone marrow. On T2-weighted images signal intensity is variable, with extravertebral masses being better identified on T2-weighted images and greater conspicuousness of intravertebral lesions on fat suppression or short tau inversion recovery (STIR) sequences. Intravenous contrast injection reveals typically diffuse enhancement in lytic lesions [1]. Considering the sclerotic rim of the singular lesion, appearing as bone remodeling of the lumbar and sacral vertebrae, a metastasis was not very likely in the present patient.

Meningioma

Meningiomas are typically slow-growing, benign (90–95% WHO grade I), intradural extramedullary masses, most of-

ten located in the thoracic spine, followed by the cervical spine and rarely occurring in the lumbosacral spine. Approximately 80% of patients are female with a peak incidence in the fifth and sixth decades of life. Meningiomas arise from arachnoid cap cells and present typically round or oval-shaped. They show broad dural attachment and a dural tail may be present. The CT findings may be calcifications, rarely bony remodeling. On non-enhanced CT they are most often occult because of similar attenuation to the spinal cord. The MRI signal intensity on T1 and T2-weighted images is typically isointense (sometimes hyperintense) to the spinal cord. On T2-weighted images calcified areas may be hypointense, cystic degeneration would be hyperintense. Hemorrhage is uncommon. On contrast-enhanced CT and MRI meningiomas typically show a strong, diffuse enhancement [4, 5]. Because of the rare lumbosacral location, inhomogeneous and partially T2-weighted hyperintense signal, patchy contrast enhancement and advanced bone remodeling, a meningioma appears unlikely, although cases of meningiomas with unusual contrast enhancement have been reported [5].

Myxopapillary Ependymoma

The rare myxopapillary subtype of ependymoma (27–30% of all ependymomas) is a slow-growing, WHO grade I, extramedullary tumor arising from ependymal cells of the conus, filum terminale and cauda equina with a peak incidence in patients 30–40 years of age. Slow tumor growth may lead to delayed diagnosis. The lesion is well circumscribed and typically spans 2–4 or more vertebral segments and may fill the entire lumbosacral spinal canal, compress the nerve roots of the cauda equina or expand along the neuroforamina. Depending on tumor size a bone remodeling occurs with expansion of the vertebral canal, thinning of pedicles and scalloping of vertebrae. The tumor may present with a heterogeneous signal related to local hemorrhages. Typically, there is isointense or hyperintense signal to spinal cord in T1-weighted images because of mucin accumulation and almost always hyperintense signal in T2-weighted images. Contrast enhancement is intense and often heterogeneous because of hemorrhages, mucinous areas and tumor necrosis [6–8].

In the present case, the diagnosis of a myxopapillary ependymoma seems very likely, with almost all imaging criteria, such as bone remodeling, hemorrhage and heterogenous signal and enhancement, are fulfilled.

Paraganglioma

Paragangliomas are benign (WHO grade I), slow-growing neuroendocrine tumors arising from neural ectoderm with an unusual spinal localization representing approximately 3.5–4% of all neoplasms at the level of the cauda equina. Paragangliomas appear at any age and often show chronic, unspecific clinical symptoms, such as back pain or radiculopathy. The tumors are hypervascular and intradural extramedullary expanding with possible bony remodeling of large tumors. Size is variable with small ovoid to round masses up to a span of four or more vertebral segments. The MRI features are isointense to hypointense signal relative to spinal cord in T1-weighted images. The T2-weighted images show very heterogeneous signals with cystic areas, hemorrhages or hemosiderin rim as well as prominent flow voids representing enlarged draining veins. Contrast enhancement ranges from intense homogeneous to heterogeneous [9, 10]. In summary, predominant radiological features are the same for myxopapillary ependymoma and paraganglioma, making them radiologically indistinguishable. In conclusion, a paraganglioma would be another possible, although very rare diagnosis in the present case.

Schwannoma

Schwannomas occur in middle-aged patients between 30–60 years, are well circumscribed, encapsulated, round to lobulated benign (WHO grade I) neoplasms of the myelinated nerve sheath (Schwann cells). Most of these are localized intradural and extramedullary. Approximately 30% of schwannomas show intradural and extradural components with extension through the neuroforamina and a “dumbbell” appearance. Size varies from small intradural masses to large intraspinal or paravertebral masses. They often appear at the lumbosacral spine. Most common is a sporadic occurrence but patients with history of neurofibromatosis 2 (NF2) often suffer from multiple schwannomas in combination with meningiomas and ependymomas. Large intraspinal or intraforaminal tumors may cause bony remodeling, typically with widening of the neuroforamen. The MRI appearance is mostly isointense to hypointense to the spinal cord on T1-weighted images and mostly hyperintense on T2-weighted images. Some tumors show cystic components, hemorrhage is rare but may be seen. Contrast enhancement may be intense but heterogeneous or merely a peripheral rim pattern can be observed [11–13]. In this case a giant schwannoma would also be a possible diagnosis as signal intensities in T1 and T2-weighted images as well as heterogeneous enhancement and hemorrhages match; however, the predominantly intraspinal and only minimal transforaminal tumor extension appears to be less typical.

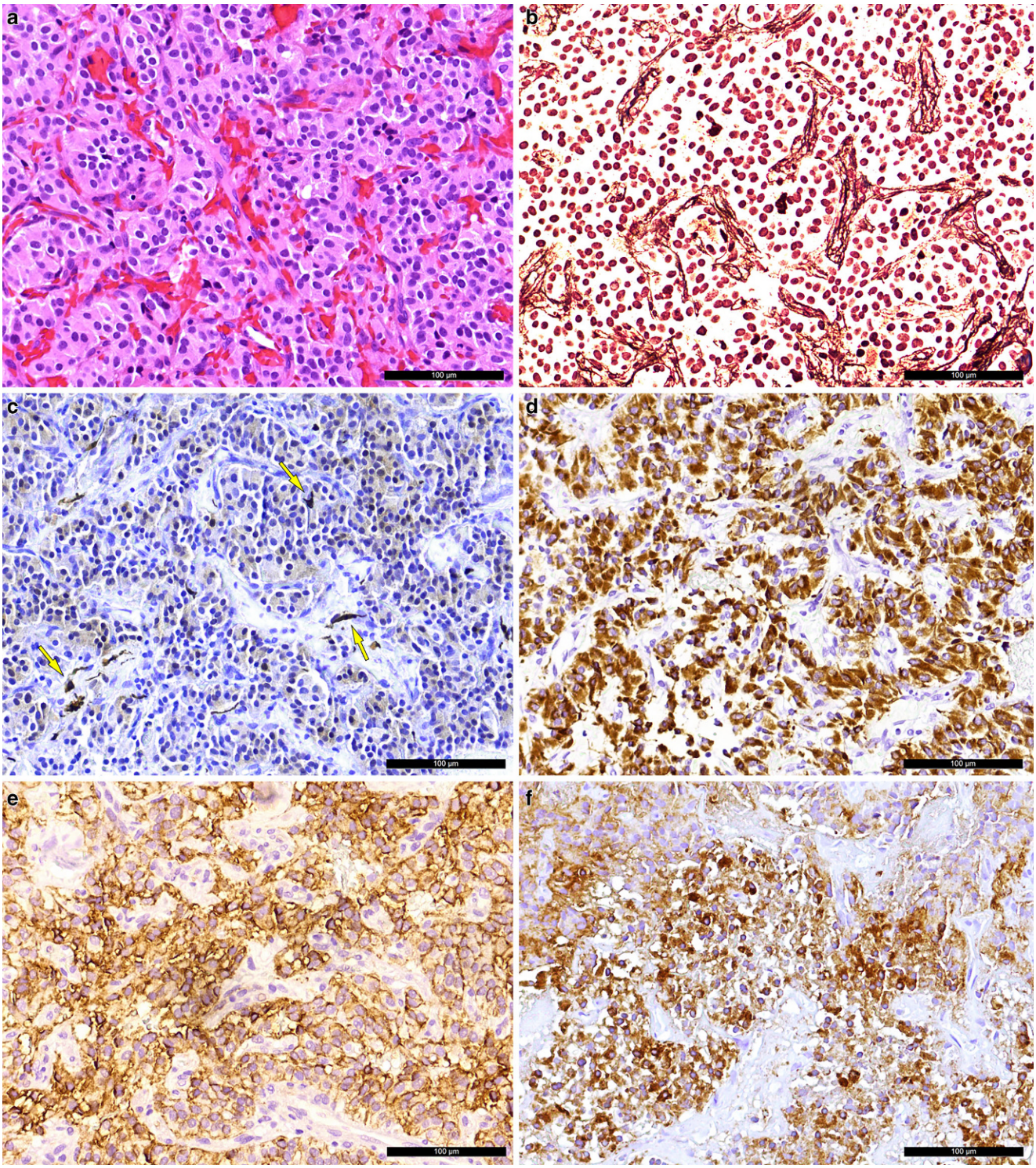

Fig. 3 Hematoxylin and eosin (H&E) stain (**a**) show a tumor with a moderate cell density. In some areas extensive bleeding can be observed. The cells are arranged in lobules or nests. On reticulin silver staining (Tibor-PAP, **b**) lobules are surrounded by a delicate reticulin fiber network. Immunohistochemical staining for S100 (**c**) shows cells with a spindle-like shape (*arrows*). These cells partially have long processes. The cells are partially labelled by the pan-cytokeratin marker (**d**) MNF116 (PanCK, *brown*). Most of the cells are positive in the immunohistochemical reaction for CD56 (**e**, *brown*). Tumor cells reacted positive in the immunohistochemical reaction for synaptophysin (**f**, *brown*)

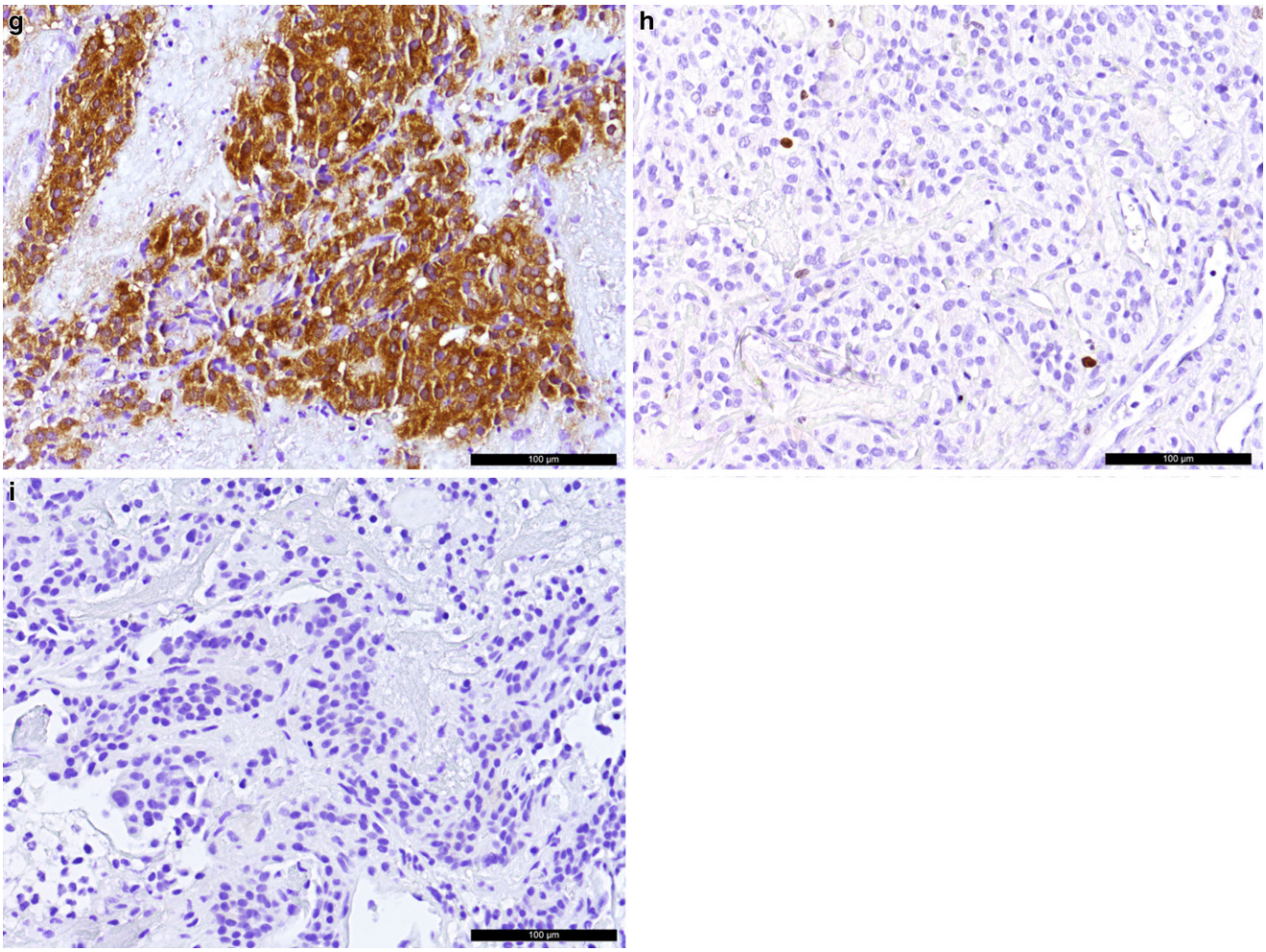

Fig. 3 (continued) The cells are also labelled in the immunohistochemical staining for neuron-specific enolase (**g**, *brown*). In total, immunohistochemical staining for Ki-67 (**h**) labelled about 1% of the cells as proliferative (*brown*). The immunohistochemical reactions for CK5/6, CK7, CK20, thyroid transcription factor 1 (TTF1), prostate-specific antigen (PSA) and epithelial membrane antigen (EMA) were negative (**i**). All images were taken with a 20× objective. Hematoxylin (*blue*) was used as counterstaining in immunohistochemical reactions. The scale bar represents 100 µm

Histology

A biopsy of an intraspinal tumorous growth was obtained for intraoperative pathological analysis. Microscopically, hematoxylin and eosin (H&E) staining from frozen cryostat sections showed blood, single leucocytes and small parts of connective tissue. After further surgical preparation, tumor masses located in the ventral portion of the spinal epidural space were reached. In situ, the tumorous growth bled freely. A second tissue specimen was obtained for intraoperative pathological analysis. The H&E staining revealed a tumor with an epithelioid, lobulated growth pattern with relatively isomorphic cytoplasm-rich cells. These findings led to the initial intraoperatively suspected diagnosis of a carcinoma metastasis. Additional biopsy material was obtained that was fixed in formaldehyde and embedded in paraffin. The H&E stained sections showed a tumor with a moderate cell density, extensive bleeding in some areas and a lobulated growth pattern. The cells were arranged in lobules or nests, so-called *Zellballen* (Fig. 3a). The *Zellballen* were surrounded by a reticulin fiber network, which could be visualized in a reticulin silver staining (Tibor-PAP, Fig. 3b). The tumor cells had central, mostly round nuclei with finely stippled or compact chromatin and a light eosinophilic cytoplasm. There was no elevated mitotic index. Furthermore, no necrotic areas were observed.

Immunohistochemical staining for S100 marked spindle-shaped cells (Fig. 3c). These cells surrounded the *Zellballen*, partially had long processes and are known as sustentacular cells. The tumor cells were partially labelled by the pan-cytokeratin marker MNF116 (PanCK, Fig. 3d). Most of the tumor cells were positive in the immunohistochemical reaction for CD56 (Fig. 3e). Positive signal was also observed in the reactions for synaptophysin (Fig. 3f)

and neuron-specific enolase (NSE, Fig. 3g). The immunohistochemical reactions for the cytokeratins CK5/6, CK7 and CK20 were negative (Fig. 3i). Moreover, the tumor cells reacted negatively in the immunohistochemical staining for thyroid transcription factor 1 (TTF1), prostate-specific antigen (PSA) and epithelial membrane antigen (EMA). Only a few blood vessels were labelled in the immunohistochemical reaction for CD34. Some infiltrating leucocytes were shown by immunohistochemical staining for leucocyte common antigen (LCA). In total, staining for Ki-67 (Mib1) labelled about 1% of the cells as being proliferative (Fig. 3h).

Based on the histological and immunohistochemical findings, several differential diagnoses were discussed including a metastasis of a neuroendocrine tumor. Given a neuroendocrine differentiation, PanCK positivity, and TTF1 negativity, the findings could have been compatible with a neuroendocrine neoplasm of the digestive system. With a low mitotic index and a proliferation rate lower than 2% in the immunohistochemical staining for Ki-67, the findings would correspond to a neuroendocrine tumor (NET) grade G1, also known as carcinoid [14]. Therefore, additional immunohistochemical staining for EP4 and CDX2 were performed but showed negative results. In addition, an exclusive intraspinal manifestation and the detection of S100 positive spindle-shaped cells argue against the presence of a neuroendocrine tumor. Instead, the results correspond to the characteristic features of a paraganglioma [15]: tumor masses bled freely; tumor cells showed immunoreactivity for neuroendocrine markers such as synaptophysin or NSE; sustentacular cells were spindle-shaped, S100 positive, and surrounded *Zellballen* that could be visualized by reticulin silver staining. Furthermore, paragangliomas arising from the cauda equina are known to show positivity for cytokeratins [16].

Diagnosis

Paraganglioma

Paraganglioma is defined by the WHO classification of tumors of the central nervous system as a unique neuroendocrine neoplasm that arises in specialized neural crest cells associated with segmental or collateral autonomic ganglia or paraganglia [15]. Histological key features of this entity include nest-like structures (*Zellballen*) that are surrounded by sustentacular cells and a fine capillary network. Paraganglioma is graded as WHO grade I.

The entity is uncommon in the central nervous system. With over 300 cases reported since the 1970s, the most common localization is the cauda equina/filum terminale. The tumor affects adults, predominantly males. While a single paraganglioma is thought to be benign, multiple paragangliomas or a co-occurrence with other neoplasms, such as renal cancer or pituitary tumors, indicate a genetic predisposition and should be assessed accordingly [17].

Compliance with ethical guidelines

Conflict of interest C.A. Taschner, M. Schwabenland, U. Hubbe, H. Urbach, A. Stadler and M. Prinz declare that they have no competing interests.

Ethical standards All investigations described in this manuscript were carried out with the approval of the responsible ethics committee and in accordance with national law and the Helsinki Declaration of 1975 (in its current revised form). Informed consent was obtained from the patient's legal representatives in this case if identifiable from images or other information within the manuscript.

References

1. Guillevin R, Vallee JN, Lafitte F, Menuel C, Duverneuil NM, Chiras J. Spine metastasis imaging: review of the literature. J Neuroradiol. 2007;34:311–21.
2. Maccauro G, Spinelli MS, Mauro S, Perisano C, Graci C, Rosa MA. Physiopathology of spine metastasis. Int J Surg Oncol. 2011;2011:107969.
3. Quraishi NA, Giannoulis KE, Edwards KL, Boszczyk BM. Management of metastatic sacral tumours. Eur Spine J. 2012;21:1984–93.
4. Liu WC, Choi G, Lee SH, Han H, Lee JY, Jeon YH, Park HS, Park JY, Paeng SS. Radiological findings of spinal schwannomas and meningiomas: focus on discrimination of two disease entities. Eur Radiol. 2009;19:2707–15.
5. Yoshiura T, Shrier DA, Pilcher WH, Rubio A. Cervical spinal meningioma with unusual MR contrast enhancement. AJNR Am J Neuroradiol. 1998;19:1040–2.
6. Sun B, Wang C, Wang J, Liu A. MRI features of intramedullary spinal cord ependymomas. J Neuroimaging. 2003;13:346–51.
7. Menzilcioglu MS, Sahin T, Citil S. A rare case of extramedullary myxopapillary ependymoma. Spine J. 2015;15:367.
8. Kahan H, Sklar EM, Post MJ, Bruce JH. MR characteristics of histopathologic subtypes of spinal ependymoma. AJNR Am J Neuroradiol. 1996;17:143–50.
9. Corinaldesi R, Novegno F, Giovenali P, Lunardi T, Floris R, Lunardi P. Paraganglioma of the cauda equina region. Spine J. 2015;15:e1–8.
10. Mishra T, Goel NA, Goel AH. Primary paraganglioma of the spine: a clinicopathological study of eight cases. J Craniovertebr Junction Spine. 2014;5:20–4.
11. Yu NH, Lee SE, Jahng TA, Chung CK. Giant invasive spinal schwannoma: its clinical features and surgical management. Neurosurgery. 2012;71:58–66.
12. Friedman DP, Tartaglino LM, Flanders AE. Intradural schwannomas of the spine: MR findings with emphasis on contrast-enhancement characteristics. AJR Am J Roentgenol. 1992;158:1347–50.
13. Liu WC, Choi G, Lee SH, Han H, Lee JY, Jeon YH, Park HS, Park JY, Paeng SS. Radiological findings of spinal schwannomas and meningiomas: focus on discrimination of two disease entities. Eur Radiol. 2009;19:2707–15.
14. Rindi G, Arnold R, Bosman FT, Capella C, Klimstra DS, Klöppel G, Komminoth P, Solcia E. Nomenclature and classification of neuroendocrine neoplasms of the digestive system. In: WHO Classification of Tumours of the Digestive System. 4th ed. 2010.

15. Brandner S, Soffer D, Stratakis CA, Yousry T. Paraganglioma. In: Louis DN, Ohgaki H, Wiestler OD, Cavenee WK, editors. WHO classification of tumors of the central nervous system. 4th ed. Lyon: IARC; 2016.
16. Chetty R. Cytokeratin expression in cauda equina paragangliomas. Am J Surg Pathol. 1999;23:491.
17. Gupta S, Zhang J, Milosevic D, Mills JR, Grebe SK, Smith SC, Erickson LA. Primary renal Paragangliomas and renal neoplasia associated with Pheochromocytoma/Paraganglioma: analysis of von Hippel-Lindau (VHL), Succinate Dehydrogenase (SDHX) and Transmembrane protein 127 (TMEM127). Endocr Pathol. 2017;28:253–68.